Proceedings of the 2003 IEEE/ASME
International Conference on
Advanced Intelligent Mechatronics (AIM 2003)

Emergency Path Planning for Autonomous Vehicles Using Elastic Band Theory

Jens Hilgert†, Karina Hirsch†, Torsten Bertram‡ and Manfred Hiller†

† Institute of Mechatronics and System Dynamics
Faculty of Engineering
Gerhard Mercator University Duisburg
Germany
Email: hilgert@imech.de

‡ Mechatronics Laboratory
Faculty of Mechanical Engineering
Ilmenau Technical University
Germany

Abstract— **In this paper a path planning method for emergency maneuvers of autonomous vehicles is presented. The path planning method is based on the theory of elastic bands. Due to the local disturbances caused by obstacles on the nominal trajectory the elastic behavior allows sufficient flexibility of the emergency trajectory and minimal local changes of curvature. The minimization of local changes of curvature ensures the driveability of the emergency trajectory under vehicle dynamics aspect, which is also considered in this paper. The results of the described method is demonstrated for emergency situations in lane change maneuvers for autonomous vehicles.**

I. Introduction

The current research in the automotive field focuses more and more on the development of automated vehicles with autonomous functions [1]. The aim of this development process is a completely Autonomous Guided Vehicle (AGV). AGVs constitute the base for a future Intelligent Transportation System (ITS) [2]. Such intelligent transportation systems are expected to improve safety, efficiency, and accessibility of transit and quality of highway travel. Due to the risk of road traffic the safety demands on the development of such autonomous systems are very high. Therefore the main requirement for future AGVs is to ensure the safety of the driver and the vehicles.

A. Problem Description

To guarantee the safety the vehicle controller should always simultaneously plan a nominal and an emergency trajectory. With the help of this planning process the vehicle controller is able to provide an emergency trajectory before and during the performance of a lane change or any other maneuver. In the case of a maneuver abortion the vehicle is immediately able to switch to the emergency trajectory. To ensure the safety of the vehicle the feasibility of the planed paths under the given conditions is essential, i.e. the vehicle velocity, the vehicle performance and the road conditions.

B. Previous Work

The emergency path planning method presented in this paper is based on a previously developed path planning method for nominal trajectories [3]. The method used permits the inclusion of vehicle dynamics aspects into the autonomous vehicles path planning process. The path planning technique for nominal trajectories was based on a Bézier spline description of the path. Furthermore optimizations with respect to driving maneuvers were performed and a method to a priori calculated the dynamic behavior of the vehicle during the maneuver was developed and will be used in the paper.

In section two a vehicle model which is used by the path planning algorithm is introduced. The path planning algorithm that combines the geometrical aspects of path planning with vehicle dynamics is presented in section three. Section four describes the basic ideas of the elastic band. The trajectory planning is presented in section five. Simulation results are discussed in section five followed by a summary of the paper including an outlook.

II. Vehicle Model

To ensure the feasibility of the emergency path some basics of vehicle dynamics have to be considered. In this section a simplified vehicle model for lateral and yaw vehicle dynamics is described. Figure 1 shows a schematic of half of a vehicle known as bicycle model [4].

As shown in Fig. 1 the important state variables are: the yaw angle $\psi(t)$, the longitudinal velocity $w(t)$ and the lateral velocity $v(t)$. The steering angle of the car is denoted as $\delta(t)$[1].

A simple two degree of freedom model for the vehicle with mass m and moment of inertia I_{zz} given in (2) and (3) is used to describe the lateral dynamics of the vehicle. The equations for the linearized model are derived from Fig. 1.

[1]Time arguments are neglected in the following.

0-7803-7759-1/03/$17.00 © 2003 IEEE

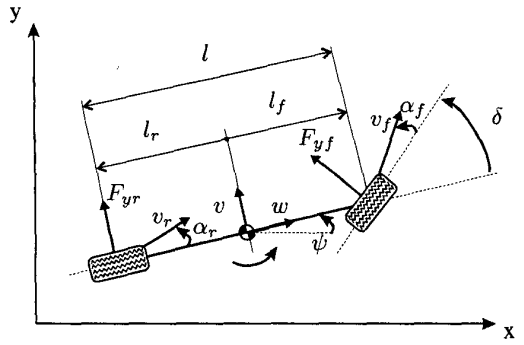

Fig. 1. Bicycle model

The cornering stiffness of the front tires is described by C_f and of the rear tires by C_r. In this case the relationship between the slip angle α and the lateral tire force F_y is assumed to be linear for the whole slip angle range. Hence the lateral tire force at front and rear axel can be described as:

$$F_{yf} = C_f\,\alpha_f \quad \text{and} \quad F_{yr} = C_r\,\alpha_r\,. \tag{1}$$

With $C = C_f + C_r$ and $C_l = C_f l_f - C_r l_r$ and the linear tire model the linearized equations are[2]

$$m\left(\dot{v} + w\,\dot{\psi}\right) + \frac{C}{w}\,v + \frac{C_l}{w}\,\dot{\psi} = C_f\,\delta \tag{2}$$

and with $C_{l^*} = C_f l_f^2 + C_r l_r^2$

$$I_{zz}\,\ddot{\psi} + \frac{C_{l^*}}{w}\,\dot{\psi} + \frac{C_f l_f - C_r l_r}{w}\,v = C_f\,l_f\,\delta \quad . \tag{3}$$

The vehicle path of the position of the center of gravity is calculated by integrating the accelerations a_x and a_y from the fixed coordinate system x-y described by:

$$\begin{bmatrix} a_x \\ a_y \end{bmatrix} = \begin{bmatrix} \cos\psi & -\sin\psi \\ \sin\psi & \cos\psi \end{bmatrix} \begin{bmatrix} \dot{u} - v\,\dot{\psi} \\ \dot{v} + u\,\dot{\psi} \end{bmatrix} \quad . \tag{4}$$

It has been confirmed that under normal driving conditions (below 0.4g lateral acceleration) the two degree of freedom bicycle model with linear tire model is completely adequate to the nonlinear vehicle behavior [5].

III. The Principle of the Elastic Band

The theory of elastic bands was original used to determine collision free paths within varying environments [6]. For the sake of completeness the ideas of the theory will briefly be discussed in this section. The interaction between a node and its neighbors is implemented on a force level. To model the contraction forces the elastic band internal contraction forces are introduced, which are based on potential spring forces (see Fig. 2). The corresponding spring potential, with spring constant c_{int} of the whole band can be written:

$$P_{int}(\mathbf{r}_0, \mathbf{r}_1, \ldots, \mathbf{r}_n) = c_{int} \sum_{k=0}^{n-1} \|\mathbf{r}_{k+1} - \mathbf{r}_k\|\,, \tag{5}$$

[2]The longitudinal velocity w is assumed to be constant.

where $\mathbf{r}_k, k = 0, 1, \cdots, n$ represents the vector from the inertia frame to the nodes k.

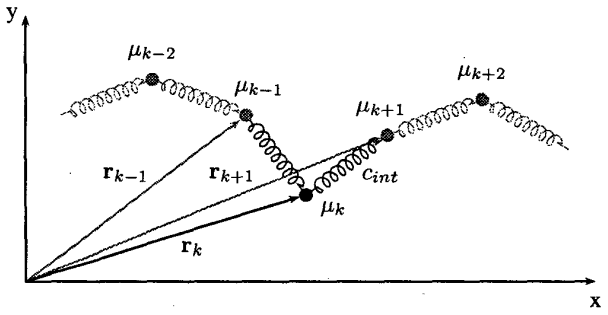

Fig. 2. Internal contraction forces

Derivation of the spring potential with respect to $\mathbf{r}_k$ yields the spring forces, $\mathbf{F}_{int,k}$, at each node $k = 1, \cdots, n-1$:

$$\mathbf{F}_{int,k} = -c_{int}\left(\frac{\mathbf{r}_k - \mathbf{r}_{k-1}}{\|\mathbf{r}_k - \mathbf{r}_{k-1}\|} + \frac{\mathbf{r}_{k+1} - \mathbf{r}_k}{\|\mathbf{r}_{k+1} - \mathbf{r}_k\|}\right)\,. \tag{6}$$

The inertial force $\mathbf{F}_{int,k}$ guarantees that the tension in the band when it is in equilibrium is equal everywhere. The elastic band should also react to obstacles (see Fig. 3). Therefore a repulsive nonlinear potential for the whole band is formulated ($\mathbf{d}_k = \mathbf{r}_k - \mathbf{r}_{obst}$):

$$P_{ext}(\mathbf{r}_0, \mathbf{r}_1, \ldots, \mathbf{r}_n) = \sum_{k=1}^{n} \begin{cases} \frac{c_{ext}}{2}(d_0 - \|\mathbf{d}_k\|)^2\,; \|\mathbf{d}_k\| < d_0 \\ 0 \qquad\qquad\quad ; \text{otherwise}\,. \end{cases} \tag{7}$$

The external potential force is calculated as the negative gradient of the potential P_{ext}:

$$\mathbf{F}_{ext,k} = \begin{cases} c_{ext}(d_0 - \|\mathbf{d}_k\|)\frac{\mathbf{d}_k}{\|\mathbf{d}_k\|} & ; \quad \|\mathbf{d}_k\| < d_0 \\ 0 & ; \quad \text{otherwise}\,. \end{cases} \tag{8}$$

The resulting force acting at a node k is the sum of the internal and external forces:

$$\mathbf{F}_{total,k} = \mathbf{F}_{int,k} + \mathbf{F}_{ext,k} \quad ; \quad k = 0, 1, \ldots, n\,. \tag{9}$$

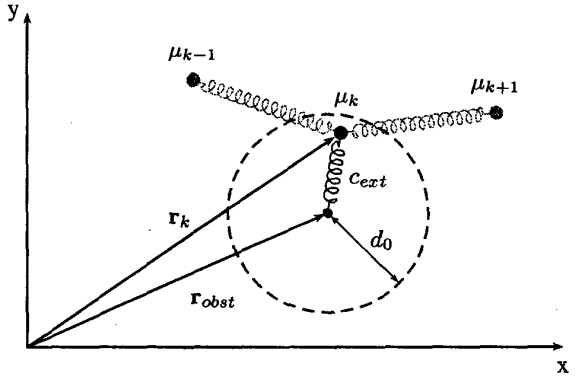

Fig. 3. External forces

With the balance of forces the equations of motion for each discrete point $\mu_0, \ldots, \mu_n$ can be written as:

$$\left.\begin{array}{ccccccc} & & \mathbf{F}_{int_{0,1}} & + & \mathbf{F}_{ext_0} & = & \mu_1\ddot{\mathbf{r}}_0 \\ & & \vdots & & \vdots & & \vdots \\ \mathbf{F}_{int_{k,k-1}} & + & \mathbf{F}_{int_{k,k+1}} & + & \mathbf{F}_{ext_k} & = & \mu_k\ddot{\mathbf{r}}_k \\ \vdots & & \vdots & & \vdots & & \vdots \\ \mathbf{F}_{int_{n,n-1}} & & & + & \mathbf{F}_{ext_n} & = & \mu_n\ddot{\mathbf{r}}_n \end{array}\right\}, \quad (10)$$

for $k = 1, 2, \ldots, n-1$. For the emergency path planning the dynamics of the elastic band can be neglected. In this paper a static model of the elastic band is used, i.e. $\dot{\mathbf{r}}_k = \ddot{\mathbf{r}}_k = \mathbf{0}$, $k = 0, 1, \ldots, n$. The equations of motion (10) of the elastic band can therefore be written as:

$$\left.\begin{array}{ccccc} & \mathbf{F}_{int_{0,1}} & = & -\mathbf{F}_{ext_0} \\ & \vdots & & \vdots \\ \mathbf{F}_{int_{k,k-1}} + & \mathbf{F}_{int_{k,k+1}} & = & -\mathbf{F}_{ext_k} \\ \vdots & \vdots & & \vdots \\ \mathbf{F}_{int_{n,n-1}} & & = & -\mathbf{F}_{ext_n} \end{array}\right\}, \quad (11)$$

for $k = 1, 2, \ldots, n-1$. At the node μ_k the internal forces can now be written with the displacement $\mathbf{u}_k$ as:

$$\left.\begin{array}{l} \mathbf{F}_{int_{k,k-1}} = c_{int}(\mathbf{u}_k - \mathbf{u}_{k-1}), \quad k = 1, \ldots, n \\ \mathbf{F}_{int_{k,k+1}} = c_{int}(\mathbf{u}_k - \mathbf{u}_{k+1}), \quad k = 0, \ldots, n-1 \end{array}\right\} \quad (12)$$

in the direction of the neighbored nodes μ_{k-1} and μ_{k+1}, whereby the boundary conditions are

$$\mathbf{u}_0 = \mathbf{0} \quad \text{and} \quad \mathbf{u}_n = \mathbf{0} \quad . \quad (13)$$

The new position $\mathbf{r}_k^{new}$, $k = 0, 1, \ldots, n$, of the nodes $\mu_0, \mu_1, \ldots, \mu_n$ can be calculated by

$$\mathbf{r}_k^{new} := \mathbf{r}_k^{old} + \mathbf{u}_k, \quad k = 0, 1, \ldots, n, \quad (14)$$

with the original position $\mathbf{r}_k^{old}$, $k = 0, 1, \ldots, n$ and the displacements $\mathbf{u}_0, \mathbf{u}_1, \ldots, \mathbf{u}_n$. In Fig. 4 an example of the elastic behavior with one and three obstacles is shown.

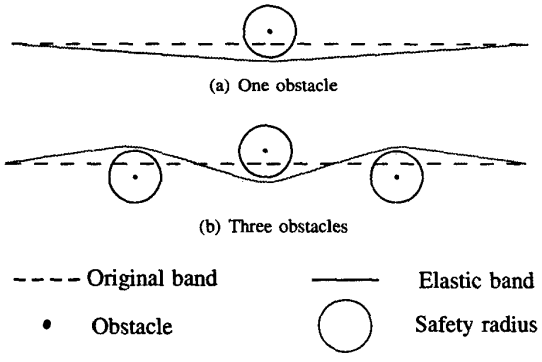

Fig. 4. Behavior of an elastic band

IV. Trajectory Planning

The nodes $\mu_0, \mu_1 \ldots, \mu_n$ of the elastic band will now be interpolated by a cubic spline curve [7],[8]. The spline curve $\mathbf{x}(u)$ is defined for $u \in [0, 1]$. In order to calculate the parameters of the tag points $u_0, u_1, \ldots, u_n$ belonging to the interpolation points[3] $\mathbf{P}_0, \mathbf{P}_1, \ldots, \mathbf{P}_n$, which fix

$$0 = u_0 < \ldots < u_n = 1 \quad \text{und} \quad \mathbf{x}(u_i) = \mathbf{P}_i, \quad (15)$$

with $i = 0, 1, \ldots, n$, several solutions are possible. In this paper the parameters are defined by

$$u_i = \frac{1}{s}\sum_{j=0}^{i} d_j, \quad i = 0, 1, \ldots, n, \quad (16)$$

whereas

$$d_0 := 0, \quad d_i = \sqrt{\|\mathbf{P}_i - \mathbf{P}_{i-1}\|_2}, \quad i = 1, 2, \ldots, n \quad (17)$$

describe the distances between the tag points and

$$s = \sum_{i=1}^{n} d_j, \quad (18)$$

the total length of the polygon belonging to the tag points.

The curve consists of n cubic polynom segments $\mathbf{x}_i$, $i = 0, 1, \ldots, n-1$, which connect the neighboring points $\mathbf{P}_i$ und $\mathbf{P}_{i+1}$ with each other. For the sake of clarity the length of an interval $[u_i, u_{i+1}]$, $i = 0, 1, \ldots, n-1$, will be noted as $\triangle u_i := u_{i+1} - u_i$ with $i = 0, 1, \ldots, n-1$ in the following. For the determination of a parameter description of the curve segment $\mathbf{x}_i$ the following equation

$$\mathbf{x}_i(u) = \mathbf{a}_i(u - u_i)^3 + \mathbf{b}_i(u - u_i)^2 + \mathbf{c}_i(u - u_i) + \mathbf{d}_i, \quad (19)$$

with $u \in [u_i, u_{i+1}]$, will be chosen as approach. Due to the twice differentiability of the interpolation curve, within the transitions of the segment $\mathbf{P}_i$, $i = 1, 2, \ldots, n-1$, the function values, the gradients and the second derivatives have to match:

$$\left.\begin{array}{rcl} \mathbf{x}_i(u_i) & = & \mathbf{x}_{i-1}(u_i) \\ \mathbf{x}'_i(u_i) & = & \mathbf{x}'_{i-1}(u_i) \\ \mathbf{x}''_i(u_i) & = & \mathbf{x}''_{i-1}(u_i) \end{array}\right\} \quad (20)$$

or

$$\left.\begin{array}{rcl} \mathbf{x}_i(u_{i+1}) & = & \mathbf{x}_{i+1}(u_{i+1}) \\ \mathbf{x}'_i(u_{i+1}) & = & \mathbf{x}'_{i+1}(u_{i+1}) \\ \mathbf{x}''_i(u_{i+1}) & = & \mathbf{x}''_{i+1}(u_{i+1}) \end{array}\right\}. \quad (21)$$

The integration of this conditions into (19) yields

$$\left.\begin{array}{rcl} \mathbf{x}_i(u_i) & = & \mathbf{d}_i \\ \mathbf{x}_i(u_{i+1}) & = & (\triangle u_i)^3\mathbf{a}_i + (\triangle u_i)^2\mathbf{b}_i + \\ & & + \triangle u_i\mathbf{c}_i + \mathbf{d}_i \\ \mathbf{x}'_i(u_i) & = & \mathbf{c}_i \\ \mathbf{x}'_i(u_{i+1}) & = & 3(\triangle u_i)^2\mathbf{a}_i + 2\triangle u_i\mathbf{b}_i + \mathbf{c}_i \end{array}\right\}. \quad (22)$$

where $\mathbf{x}_i(u_i) = \mathbf{P}_i, \mathbf{x}_i(u_{i+1}) = \mathbf{P}_{i+1}, \mathbf{x}'_i(u_i) = \mathbf{P}'_i$ and $\mathbf{x}'_i(u_{i+1}) = \mathbf{P}'_{i+1}$. The gradient in the interpolation points

[3]Described in the fixed coordinate system x-y.

will be denoted by $\mathbf{P'}_i$, $i = 0, 1, \ldots, n$, which are unknown so far. Now the coefficients are determined by (21) and (22):

$$\left.\begin{array}{rcl} \mathbf{a}_i & = & \frac{\left(2(\mathbf{P}_i - \mathbf{P}_{i+1}) + \Delta u_i(\mathbf{P'}_i + \mathbf{P'}_{i+1})\right)}{(\Delta u_i)^3} \\ \mathbf{b}_i & = & \frac{\left(-3(\mathbf{P}_i - \mathbf{P}_{i+1}) - \Delta u_i(2\mathbf{P'}_i + \mathbf{P'}_{i+1})\right)}{(\Delta u_i)^2} \\ \mathbf{c}_i & = & \mathbf{P'}_i \\ \mathbf{d}_i & = & \mathbf{P}_i \end{array}\right\} . \quad (23)$$

With (19) the cubic splines curve between $\mathbf{P}_i$ and $\mathbf{P}_{i+1}$, $i = 0, 1, \ldots, n-1$, with respect to the interval $[0, 1]$, is given by:

$$\begin{aligned} \mathbf{x}_i(u) = & \left(2\tfrac{(u-u_i)^3}{(\Delta u_i)^3} - 3\tfrac{(u-u_i)^2}{(\Delta u_i)^2} + 1\right)\mathbf{P}_i + \\ & + \left(-2\tfrac{(u-u_i)^3}{(\Delta u_i)^3} + 3\tfrac{(u-u_i)^2}{(\Delta u_i)^2}\right)\mathbf{P}_{i+1} + \\ & + \left(\tfrac{(u-u_i)^3}{(\Delta u_i)^2} - 2\tfrac{(u-u_i)^2}{\Delta u_i} + u - u_i\right)\mathbf{P'}_i + \\ & + \left(\tfrac{(u-u_i)^3}{(\Delta u_i)^2} - \tfrac{(u-u_i)^2}{\Delta u_i}\right)\mathbf{P'}_{i+1} . \end{aligned} \quad (24)$$

Out of the set of curve segments $\{\mathbf{x}_0, \mathbf{x}_1, \ldots, \mathbf{x}_{n-1}\}$ the cubic spline curve is described by:

$$\mathbf{x}(u) = \left\{\begin{array}{ll} \mathbf{x}_0(u) & \text{für } u \in [u_0, u_1[\\ \vdots & \\ \mathbf{x}_{n-2}(u) & \text{für } u \in [u_{n-2}, u_{n-1}[\\ \mathbf{x}_{n-1}(u) & \text{für } u \in [u_{n-1}, u_n] \end{array}\right\} . \quad (25)$$

Within this work the gradient at the starting point and endpoint will be predefined. This specification is important because the gradient of the driven path and the starting gradient of the planned emergency path have to match in order to avoid discontinuities and therefore ensure the feasibility of the planned maneuver.

The boundary gradients are defined by the tangents in the starting point and endpoint:

$$\left.\begin{array}{rcl} \mathbf{x}'(0) & = & \mathbf{x}'_0(u_0) = \mathbf{P}'_0 =: \mathbf{T}_0 \\ \mathbf{x}'(1) & = & \mathbf{x}'_{n-1}(u_n) = \mathbf{P}'_n =: \mathbf{T}_n \end{array}\right\} . \quad (26)$$

To determine the cubic spline curve with the interpolations nodes $(u_i, \mathbf{P}_i)$, with $i = 0, 1, \ldots, n$, the given boundary gradients $\mathbf{T}_0$ and $\mathbf{T}_n$ in (26) were used in (22). Figure 5 shows the curve changes with different boundary gradients.

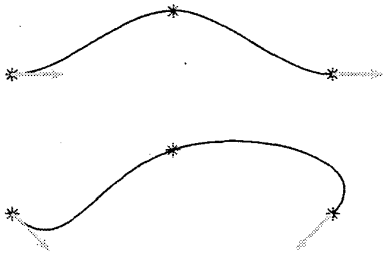

Fig. 5. Spline curves with different boundary gradients

V. Results

The results of the described method are now demonstrated for an emergency situation within a lane change maneuver of an autonomous vehicle. The nominal lane change maneuver will be disturbed by a faster vehicle coming from behind. Due to this disturbance the nominal lane change maneuver would lead to a collision between the two vehicles. In order to use the elastic band theory the vehicles are described by 6 safety areas with equal radius d_0 (see Fig. 6). Within the following simulations the safety radius is $d_0 = 1$ m.

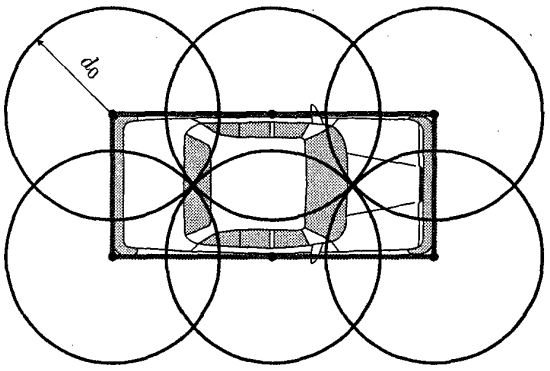

Fig. 6. Safety area definition of a vehicle

The internal contraction coefficient of the elastic band is

$$c_{int} = 1$$

and the external coefficient is

$$c_{ext} = 0.3 .$$

To ensure the feasibility of the planned emergency trajectories all driven vehicle trajectories are simulated with the described bicycle model. At this point it is important to distinguish between planned trajectories and driven trajectories based on a vehicle dynamics model. Problems like wet or icy roads in combination with high velocities require this distinction. The necessary steering angle to include the vehicle dynamics is calculated by the path planning method described in [3].

The planned and driven trajectories are shown in Fig. 7. The nominal vehicle trajectory would cause a collision between the autonomous vehicle and the faster vehicle on the lower lane. The emergency trajectory avoids the collision and turns to the lower lane behind the faster vehicle (see also Fig. 8). The autonomous vehicle in the upper lane is driving with 80 km/h and the other vehicle in the lower lane disturbing the lane change maneuver is moving with 130 km/h.

Figure 7 shows that the planned emergency trajectory is driveable with the given velocity. The lane change maneuver can be finished in spite of the disturbing vehicle. In the case that the path planning would lead to the result of an emergency

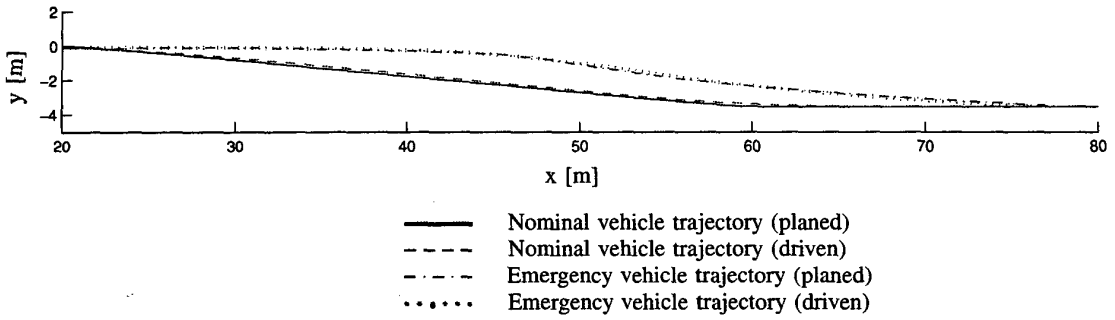

Fig. 7. Nominal and emergency trajectories

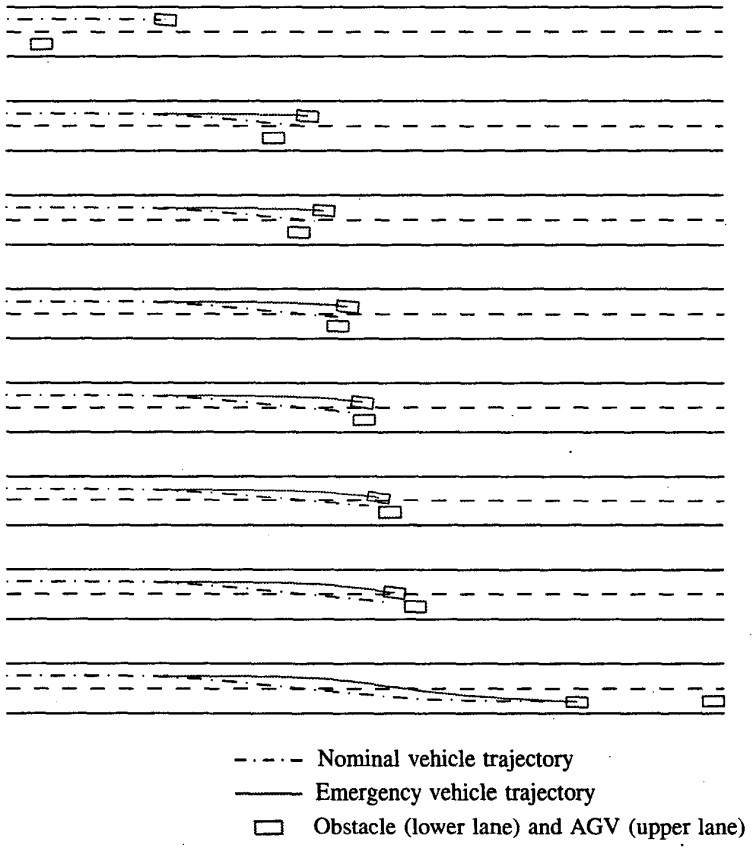

Fig. 8. Results of emergency path planning

trajectory which is not feasible under given circumstances the whole maneuver would have been aborted.

In Fig. 8 an emergency maneuver based on the described method is shown in several time steps. The additional figure

of the emergency maneuver and the depiction with time steps outlines the elastic behavior of the emergency trajectory. Especially at the point where the nominal trajectory hits the obstacle the effect of the external forces is obvious.

VI. Summary and Conclusions

In this paper a path planning method for emergency maneuvers of autonomous vehicles has been presented. The path planning method is based on the theory of elastic bands which has been summarized in the paper. The elastic behavior allows sufficient flexibility of the emergency trajectory caused by the local obstacles on the nominal trajectory. One additional objective of the path planning process is the minimization of local changes of curvature which ensures the feasibility of the emergency trajectory.

The method used permits the inclusion of vehicle dynamics into the emergency path planning process of autonomous vehicles. The advantages of including vehicle dynamics can mainly be seen in the a priori estimation of driving maneuvers. Due to this estimation, path planning methods for autonomous vehicle guidance increases the safety of the vehicle. The results of the described method are demonstrated for emergency situations in lane change maneuvers for autonomous vehicles.

One further step in the development process is to take also non-linear vehicle dynamics models into consideration. The benefit of non-linear vehicle dynamics models is to ensure the suitability of the method described for higher lateral accelerations and changing longitudinal velocities.

Another step in the development process will be the integration of a Time-To-Collision concept. With the help of this concept the external force coefficient c_{ext} can be adapted depending on the remaining time until the vehicles collide. The benefit would be a more comfortable emergency maneuver. Finally the described method will be validated with the help of a test facility using scaled vehicles [9].

Acknowledgement

The authors would like to thank the Ministry of School, Science and Research (MSWF) of the state of Nordrhein-Westfalen, Germany, for supporting this work.

References

[1] E. Dickmanns, "Vision for ground vehicles history and prospects," *Int. Journal of Vehicle Autonomous Systems*, vol. 1, no. 1, pp. 1–44, 2002.

[2] M. Bertozzi, A. Broggi, and A. Fascioli, "Vison-based intelligent vehicles: State of the art and perspectives," *Robotics and Autonomous Systems*, vol. 32, pp. 1–16, 2000.

[3] J. Hilgert and T. Bertram, "Similitude analysis for experimental validation of path planning for autonomous driving," in *Proceedings of the 2nd IFAC Conference on Mechatronic Systems*, Berkeley, California, USA, December 9-11 2002.

[4] J. Wong, *Theory of Ground Vehicles*. New York: John Wiley and Sons Inc., 1978.

[5] D. Smith and J. Starkey, "Effects of model complexity on performance of automated vehicle steering controllers: Model development, validation and comparison," *Vehicle System Dynamics*, vol. 24, no. 2, pp. 163–181, 1995.

[6] A. Komainda and M. Hiller, "Control of heavy load manipulators in varying environments," in *Proceedings of the 16th International Symposium on Automation and Robotics in Construction*, Madrid, Spain, 22-24 September 1999.

[7] J. Hoschek and D. Lasser, *Fundamentals of Computer Aided Geometric Design*. Wellesley, Massachusetts: A K Peters, 1993.

[8] G. Farin, *Curves and Surfaces for Computer Aided Geometric Design: A Practical Guide*. London: Academic Press, 1996.

[9] J. Sika, J. Hilgert, T. Bertram, J. Pauwelussen, and M. Hiller, "Test facility for lateral control of a scaled vehicel in an automated highway system," in *Proc. 8th Mechatronics Forum International Conference - Mechatronics 2002*. University of Twente, 24-26 June 2002, pp. 142–150.